COMPARISON OF THEORETICAL CALCULATION RESULTS OF THE NIGHT AIRGLOW INTENSITY WITH MEASUREMENT DATA OBTAINED BOTH BY GROUND-BASED METHODS AND FROM SPACE SHUTTLES

©2025 O.V. Antonenko *, A.S. Kirillov
Polar Geophysical Institute (PGI), Apatity (Murmansk region), Russia
**e-mail: antonenko@pgia.ru*

Received April 07, 2024
Revised September 02, 2024
Accepted October 16, 2024

The integral luminosity values of the Herzberg I, Chamberlain and Atmospheric bands at mid-latitudes and in the equatorial zone of the Earth are calculated. The correlation of the results of theoretical calculations of the intensity of excited molecular oxygen glow on Earth with experimental data on the night glow of O2 obtained from space shuttles, from the ground-based Kitt Peak Observatory (USA) for the Herzberg I and Chamberlain bands is discussed. For the Atmospheric bands, the correlation of the results of theoretical calculations with similar calculations based on measurement data from the ground-based Keck Observatory (USA) is analyzed. The integral luminosity values of the Herzberg I and Atmospheric bands for the northern latitudes of Mars are calculated.

DOI: 10.31857/S00234206250101e4

INTRODUCTION

The awareness of the possibility of upper atmosphere radiation at middle and low latitudes under quiet geomagnetic conditions did not emerge until there was an attempt to estimate the illumination of the Earth's surface at night [1]. The first such studies showed that the radiation from outer space (stars, nebulae, galaxies, zodiacal light) in the visible spectrum constitutes only a part of the total intensity of the night sky airglow [2, 3]. Modern data [4, 5] show that for the visible spectrum, the value of the total stellar radiation is about 10 kilorayleighs and about 7 kilorayleighs for the intrinsic radiation of the upper atmosphere under quiet geomagnetic conditions at middle latitudes of the Earth.

Experimental studies of the dayglow of the Martian atmosphere began during the flybys of spacecraft *Mariner-6 and Mariner-7* [6]. Measurements of the ultraviolet emission spectrum showed the presence of bands of electronically excited carbon monoxide CO and carbon dioxide ion CO_2^+ [6]. Subsequently, measurements on the spacecraft *Mars Express* discovered ultraviolet auroral emissions in the Martian atmosphere [7], which were similarly associated with CO and CO_2^+ bands.

Registration of the nightglow of the Martian atmosphere on the spacecraft *Mars Express* was mainly conducted in the infrared range [8–10]. Measurements were made for the Infrared atmospheric band at 1.27 μm, emitted during the spontaneous transition

$$O_2(a^1\Delta_g, v' = 0) \rightarrow O_2(X^3\Sigma_g^-, v'') + h\nu, (\lambda = 1.27\ \mu m). \quad (1)$$

Recently, results of measurements of the nightglow of the Martian atmosphere obtained on the spacecraft *Trace Gas Orbiter* in the visible range [11] were published. As demonstrated by the authors, the recorded spectrum coincides with measurements made on the spacecraft " *Venera9"*

and " *Venera10"* [12] and *Venus Express* [13] in the night atmosphere of Venus. The emission in the visible range is associated with Herzberg II bands of molecular oxygen, emitted during spontaneous transitions

$$O_2(c\,^1\Sigma_u^-, v' = 0) \rightarrow O_2(X\,^3\Sigma_g^-, v'') + h\nu, (\lambda = 400\text{–}650 \text{ nm}). \quad (2)$$

The processes of molecular gas dissociation by solar ultraviolet radiation in the atmospheres of terrestrial planets occur very efficiently, leading to the formation of fairly high concentrations of atomic oxygen O in the upper layers of planetary atmospheres

$$O_2 + h\nu \rightarrow O + O, \quad (3)$$

$$CO_2 + h\nu \rightarrow CO + O. \quad (4)$$

In Earth's atmosphere, the formation of atomic oxygen through process (3) occurs at altitudes above 80 km, while in the Martian atmosphere through process (4) at altitudes above 40 km. Subsequently, the formed oxygen atoms participate in triple collisions

$$O + O + M \rightarrow O_2^* + M, \quad (5)$$

where $M = N_2$, O_2 in Earth's atmosphere and $M = CO_2$ in the Martian atmosphere. As a result of such collisions (5), electronically excited oxygen molecules O_2^* are formed, capable of emitting molecular bands in various spectral ranges during spontaneous radiative transitions to lower energy states. Table 1 shows the energies of twelve vibrational levels $v = 0$–11 of five electronically excited states of the oxygen molecule. From Table 1, it can be seen that the energies of the vibrational levels of the $A\,^3\Sigma_u^+$ and $A'\,^3\Delta_u$ states have values close to the dissociation energy of the O_2 molecule (~41300 cm^{-1}), while the levels of the $b\,^1\Sigma_g^+$, $a\,^1\Delta_g$ states have much lower energy values. Electronically excited oxygen molecules emit photons, serving as a source of emission in various spectral ranges in planetary atmospheres.

The first six electronic states of O_2^* (five of which are shown in Table 1, and the sixth - quintet $^5\Pi_g$) are metastable; transitions between them cause the known nine band systems, six of which are in the ultraviolet region of the spectrum, and three are in the infrared [1]. This paper presents calculations of band intensities emitted in the night sky of Earth and Mars atmospheres during spontaneous transitions from electronically excited states $A\,^3\Sigma_u^+$, $A'\,^3\Delta_u$, $b\,^1\Sigma_g^+$, that is, the Herzberg bands I (6), the Chamberlain bands (7) and Atmospheric bands (8), respectively

$$O_2(A^3\Sigma_u^+, v') \rightarrow O_2(X^3\Sigma_g^-, v'') + h\nu, (\lambda = 240\text{–}520 \text{ nm}) \; A(A \rightarrow X) = 15 \; s^{-1}, \quad (6)$$

$$O_2(A'\,^3\Delta_u, v') \rightarrow O_2(a^1\Delta_g, v'') + h\nu, (\lambda = 300\text{–}870 \text{ nm}) \; A(A' \rightarrow a) = 0.89 \; s^{-1}, \quad (7)$$

$$O_2(b^1\Sigma_g^+, v') \rightarrow O_2(X^3\Sigma_g^-, v'') + h\nu, (\lambda = 700\text{–}1000 \text{ nm}) \; A(b \rightarrow X) = 0.087 \; s^{-1}, \quad (8)$$

with the first two band systems (6) and (7) located in the ultraviolet region, and the third (8) in the infrared. In equations (6–8) $A(A \rightarrow X)$, $A(A' \rightarrow a)$, $A(b \rightarrow X)$ are the characteristic transition probabilities (Einstein coefficients) for processes (6), (7), (8), respectively.

The purpose of this work is to compare theoretical calculations of band emission intensity, performed for both Earth's atmosphere and Mars' atmosphere, with experimental data on nightglow intensities of molecular oxygen O_2^*, obtained from space shuttles and ground stations.

The paper examines both ground-based measurements at the Kitt Peak National Observatory (USA, Arizona, 31° N, 72% clear nights), Keck Observatory (Mauna Kea peak, Hawaii Island, USA, 19° N), as well as measurements from the shuttle " *Discovery* " during its seven-day mission STS 53 in December 1992 and the shuttle *Endeavour* during its twelve-day mission STS 69 in September 1995 [14] during the Arizona Airglow experiment (GLO) . GLO is a hyperspectral thermal imager consisting of five spectrographs to record the entire spectral range. During the Arizona experiment, GLO tracked the nightglow layer at Earth's horizon [14].

PROFILES OF ATOMIC OXYGEN CONCENTRATIONS IN THE ATMOSPHERES OF EARTH AND MARS

For Earth's atmosphere, experimental data on characteristic O concentrations at middle latitudes (55.7° N; 36.8° E), based on measurements from the Zvenigorod Observatory of the Institute of Atmospheric Physics (IAP) named after A.M. Obukhov RAS), are presented in Fig. 1a for different months of the year (1 — January, 4 — April, 7 — July, 10 — October) under conditions of low ($F_{10.7}$ = 75, 1976 and 1986) solar activity [1]. For comparison, Fig. 1a also shows O concentrations obtained according to the NRLMSISE-00 atmospheric model for the conditions described above.

Experimental data on characteristic O concentrations in the equatorial region and in the northern tropics (23.5° N) of Earth (winter, spring, summer, and autumn seasons of 1995) are presented in Fig. 1b. The data were obtained through atmospheric sounding on the *TIMED* (*Thermosphere Ionosphere Mesosphere Energetics and Dynamics*) satellite [15]. The satellite used an instrument from the OSIRIS system [15]. Also, Fig. 1b shows for comparison data obtained according to the NRLMSISE-00 atmospheric model for the same conditions.

As shown in Fig. 1a and 1b, the data according to the *NRLMSISE* -00 model diverge from experimental values and are not used in calculations. For temperature profiles, data from long-term (1960 - 2000) measurements at altitudes of 30 - 110 km were used [1]. For N_2, O_2 concentration profiles, data from the MSIS-90 model were used.

Fig. 1c shows altitude profiles of O for Mars atmosphere, obtained from SPICAM IR spectrometer for orbits L_s = 152.1°, L_s = 164.5° (February, 82° S) [9] and created using the LMD-MGCM model for the same conditions (light lines) [16]. For Mars atmosphere in calculations, we will use atomic oxygen concentration profiles obtained from the French laboratory's general circulation model LMD-MGCM, shown in Fig. 1d for equatorial latitudes and 67° N of Mars, specifically for spring ($L_s \approx 0°$) and autumn ($L_s \approx 180°$) equinox conditions. For CO_2 concentration and temperature profiles, data according to the LMD-MGCM model were used [16].

CALCULATION OF O_2* CONCENTRATIONS IN THE EARTH AND MARS ATMOSPHERES

As mentioned earlier [17], when calculating concentrations of electronically excited oxygen O_2* in Earth and Mars atmospheres, we use the following formula:

$$[O_2^*] = q_{v'} \alpha k_1 [O]^2 (M_1] + ... + [M_n]) / (A_{v'} + k_2^{M1} [M_1] + ... + k_2^{Mn} [M_n), \quad (9)$$

where $q_{v'}$ is the quantum yield of vibrational level v' of electronically excited state and α is the quantum yield of this O_2^* molecule state during triple collisions (5); M_1] ... [M_n] - concentrations of predominant atmospheric gases; k_1 - rate constant of recombination reaction in triple collisions (5), which is calculated depending on the planet's atmospheric temperature at the considered altitude intervals; k_2^{M1} ... k_2^{Mn} - rate constants of quenching of electronically excited state by atmospheric components M_1 ... M_n in binary collisions; $A_{v'}$ - sum of Einstein coefficients for all spontaneous radiative transitions from vibrational level v' of O_2^* state to all vibrational levels of lower molecular states. Table 2 provides the values of formula coefficients depending on the O_2^* state and Earth or Mars conditions.

Coefficient k_1 (see ^{6} s^{-1}) for Earth's atmosphere is taken according to [1], for Mars atmosphere according to [16]. Rate constants for electronically excited oxygen reactions k_2^{O2} (cm^3 s^{-1}), k_2^{N2} (cm^3 s^{-1}) for Earth's atmosphere and, respectively, k_2^{CO2} (cm^3 s^{-1}) for

Mars atmosphere were considered according to studies [18, 19]. Quantum yields for states $A\,^3\Sigma_u^+$ ($q_{v'}^{A3}$) and $A'\,^3\Delta_u$ ($q_{v'}^{A'3}$) were considered according to works [20, 21], quantum yields for state $b\,^1\Sigma_g^+$ ($q_{v'}^{b}$) according to work [22]. Quantum yield α^{A3} and $\alpha^{A'3}$ - according to work [23], α^{b} according to [22]. The sum of Einstein coefficients $A_{v'}^{A3}$ (s^{-1}) for all spontaneous radiative transitions from vibrational level v' of state $A\,^3\Sigma_u^+$ to all vibrational levels of state $X\,^3\Sigma_g^-$ was considered according to work [24]. Similarly, the sum of coefficients $A_{v'}^{A'3}$ (s^{-1}) for all spontaneous radiative transitions from vibrational level v' of state $A'\,^3\Delta_u$ to all vibrational levels of states $a\,^1\Delta_g$ and $X\,^3\Sigma_g^-$ was also considered according to work [24]. For transitions from vibrational level v' of state $b\,^1\Sigma_g^+$ to all vibrational levels of state $X\,^3\Sigma_g^-$ values $A_{v'}^{b}$ (s^{-1}) were considered according to work [1].

COMPARISON OF EXPERIMENTAL DATA OBTAINED FROM BOTH GROUND-BASED MEASUREMENTS AND SPACE SHUTTLES WITH THEORETICAL CALCULATIONS

In this work, Fig. 2a and 3a shows a fragment of the averaged nightglow spectrum in the range of 620-900 nm, measured by a spectrograph from the space shuttle *Endeavour* during its 12-day STS mission 69 in September 1995 [14]. The radiation intensity values $I_{v'v''}$ ($cm^{-2}\ s^{-1}$) (histograms) for Atmospheric bands caused by transition (8) were calculated and presented for this wavelength range for Earth's middle latitudes in Fig. 2b. Each pair of digits above the emission peaks denotes vibrational levels ($v'-v''$) during the radiative transition (8). The radiation intensity values were also calculated for the Earth's northern tropical equator region (23.5° N) for the autumn season of 1995 (Fig. 2c). For Mars' atmosphere, histograms for Atmospheric bands were calculated for latitude 67° N at $L_s \approx 180°$ i.e., for autumn equinox (Fig. 3b).

As can be seen from the comparison of Fig. 2b and 3b, for the Martian atmosphere, there is a change in the relative populations of vibrational levels of state $b\,^1\Sigma_g^+$ and their contribution to the emission of Atmospheric bands compared to Earth's atmosphere. Thus, the population of vibrational level $v' = 1$ and $v' = 2$ relative to level $v' = 0$ significantly increases compared to Earth's atmosphere. This is explained by the different nature of quenching of this state on N_2, O_2 and CO_2 molecules [19]. The main quenching of O_2 ($b\,^1\Sigma_g^+$, $v' = 0$) molecule in Earth's atmosphere occurs on N_2 molecules, with the constant being more than two orders of magnitude lower than the similar constant for collisions with CO_2 [19]. For O_2 ($b\,^1\Sigma_g^+$, $v' = 1$) and O_2 ($b\,^1\Sigma_g^+$, $v' = 2$) molecules in Earth's atmosphere, quenching occurs on O_2 molecules, and the constants for this process exceed similar constants for collisions with CO_2. Moreover, the constant for O_2 ($b\,^1\Sigma_g^+$, $v' = 1$) + O_2 collision is an order of magnitude higher than for O_2 ($b\,^1\Sigma_g^+$, $v' = 2$) + O_2. For collisions of O_2 ($b\,^1\Sigma_g^+$, $v' = 1$) and O_2 ($b\,^1\Sigma_g^+$, $v' = 2$) with carbon dioxide molecule, the constants are close in value[19]. Therefore, there is an increase in the population of vibrational level $v' = 1$ relative to level $v' = 2$ for the Martian atmosphere.

Figure 2g also shows a fragment of the averaged night sky emission spectrum in the range of 300-870 nm, measured by a spectrograph from the space shuttle *Discovery* (STS-53) during its seven-day mission in December 1992 [14]. The calculated values of the integral luminosity of the Chamberlain bands in the same frequency range are shown in Fig. 2d for Earth's middle latitudes (55.7° N) for month 1 of 1986. Fig. 2e shows similar results for Earth's equatorial zone and northern tropics (23° N) for the winter period of 1995 . The calculations used model values of atomic oxygen concentration profiles [1, 25], obtained for mid-latitude midnight conditions based on altitude profiles of O(^{1}S) 557.7 nm emission, normalized to medium solar activity ($F_{10.7} = 130$) and undisturbed geomagnetic activity ($Kp = 0$). Comparison of calculation results with experimental data shows that both in experiment and calculations, there is a dominance of

Chamberlain bands contribution to the emission, caused by spontaneous radiative transitions (7) from vibrational levels v' = 3, 5, 6. However, the discrepancy remains unclear for the (3-4) band, for which the luminosity values in calculations appear higher compared to experimental data.

Additionally, along with experimental data obtained from space shuttles, ground-based measurement results are presented here. Fig. 4a shows the measured emission intensities of Herzberg I bands, obtained from the Ebert-Fastie spectrograph in the range of 250-370 nm (Kitt Peak National Observatory, USA, Arizona 32° N) at an altitude of 2080 m [26]. In UV wavelengths (310−450 nm), an ultraviolet low brightness source was used [27]. The observatory has been operating since 1958 , however, the authors of [26] describe observations referring to measurements from 1961−1964 during a period of low solar activity. In Fig. Figure 4b shows the calculated values of integral luminosity of the Herzberg I bands in the same frequency range for Earth's middle latitudes (55.7° N) for month 1 of 1986. Similarly, measurement data obtained from the EbertFastie spectrograph in the range of 300-870 nm, and calculated values of integral luminosity of the Chamberlain bands in the same range for Earth's middle latitudes are shown in Fig. 4c and 4d respectively.

Fig. 5 shows experimental and calculated values of integral luminosity of Atmospheric bands from the first three vibrational levels v' = 0-2 of the $b\,^1\Sigma_g^+$ state. Fig. 5a shows calculated values for Earth's middle latitudes (55.7° N) for month 1 of 1986 ; Fig. 5b shows similar measurement data obtained with the high-resolution spectrograph (HIRES) on the largest optical telescope Keck I (Keck Observatory, Mauna Kea peak, 4145 m, Hawaii, USA, 19° N) [28]; Fig. 5c shows calculation results for the equatorial zone, including northern tropics (23° N), for the winter period of 1995 . The authors of [28] note that since the aforementioned telescope first saw light, a new era began in the research of molecular oxygen O_2 Atmospheric bands system. Measurements using this telescope have been conducted since 1993; the more precise period of measurements shown in the figure is not specified, however, the author describes observations referring to works from 1994 [29], 1996 [30].

As can be seen from comparing calculation results and experimental data, the population of vibrational level v' = 0 significantly exceeds the populations of levels v' = 1 and 2, which is related to the peculiarities of quenching of these levels on N_2 and O_2 molecules [19]. In turn, the population of v' = 2 exceeds the population of v' = 1 due to lower quenching constant on O_2 molecules [19].

CONCLUSION

Based on experimental data of atomic oxygen concentration profiles and temperature in Earth's atmosphere at middle latitudes (55.7° N) and in the equatorial zone and northern tropics (23° N) for winter, spring, summer, and autumn periods, calculations of volumetric and integral intensities of Chamberlain bands in the wavelength range 300-870 nm and Atmospheric bands in the range 700-1000 nm were performed. The calculated values were compared with spectral measurements from space shuttles " *Discovery* " (STS-53) and " *Endeavour* " (STS-69) [14]. Comparison was also made with experimental data obtained from the EbertFastie spectrograph (Kitt Peak National Observatory, USA, Arizona 32° N) [26], and with data obtained using the Keck I telescope (Keck Observatory, Mauna Kea peak, 4145 m, Hawaii, USA, 19° N) [28].

It is shown that there is good correlation between calculation results and measurement data from space shuttles and ground-based measurements. Thus, radiative transitions (7) from vibrational levels v' = 3, 5, 6 of the $A'^3\Delta_u$ state provide the dominant contribution to emission in the range 300-870 nm, which agrees with experimental data. Radiative transitions (8) from vibrational levels v' = 0-2 of the $b\,^1\Sigma_g^+$ state provide the dominant contribution to emission in

the range 700-1000 nm. The radiative transitions from $b\,^1\Sigma_g$, $v' = 0$ were taken into account, which allowed identification of the 762 and 865 nm bands measured both aboard the space shuttle and using the telescope. It is shown that the calculation results agree well with data obtained from the space shuttle, but better agreement is achieved with experimental data obtained from the Keck I telescope [28].

Calculations of emission intensities of Atmospheric bands in the wavelength range 700-1000 nm were performed for Mars conditions at latitude 67° at $L_s \approx 180°$, i.e., autumnal equinox. It was found that for Mars conditions, there is a change in the relative contribution of vibrational levels of the $b\,^1\Sigma_g^+$ state to the emission of Atmospheric bands. Thus, the relative contribution of the vibrational level $v' = 1$ significantly increases compared to conditions in Earth's atmosphere. This is explained by the peculiarities of O_2 ($b\,^1\Sigma_g^+$, $v' = 0$-2) molecule quenching during collisions with the main components N_2 and O_2 in Earth's atmosphere and with CO_2 in Mars' atmosphere.

REFERENCES

1. *Shefov N.N., Semenov A.I., Khomich V.Yu.* Upper Atmosphere Emission as an Indicator of its Structure and Dynamics. Moscow: GEOS, 2006. 741 p.

2. *Newcomb S.* Is the Airship Coming? // McClure's magazine. 1901. V. 17(5). P. 432-435.

3. *Khvostikov I.A.* Night Sky Airglow. Moscow, Leningrad: USSR Academy of Sciences Publishing House, 1937. 165 p.

4. *Sharov A.S., Lipaeva N.A.* Stellar Component of Night Sky Airglow // Astron. Zhurn. 1973. V. 50. No. 1. P. 107-114.

5. *Roach F., Gordon J.* .Night Sky Airglow. Moscow: Mir, 1977. 152 p.

6. *Barth C.A., Hord C.W., Pearce J.B. et al.* Mariner 6 and 7 ultraviolet spectrometer experiment: Upper atmosphere data // J. Geophys. Res. 1971. V. 76. Iss. 10. P. 2213-2227.

7. *Bertaux J.-L., Leblanc F., Witasse O. et al.* Discovery of an aurora on Mars // Nature. 2005. V. 435. P. 790-794.

8. *Migliorini A., Altiere F., Zasova G. et al.* Oxygen airglow emission on Venus and Mars as seen by VIRTIX/VEX and OMEGA/MEX imaging spectrometers // Planet. Space Sci. 2011. V. 59. Iss. 10. P. 981-987.

9. *Fedorova A.A., Lefevre F., Guslyakova S. et al.* The O_2 nightglow in the Martian atmosphere by SPICAM onboard of Mars-Express // Icarus. 2012. V. 219. Iss. 2. P. 596-608.

10. *Bertaux J.-L., Gondet B., Lefevre F. et al* . First detection of O_2 1.27 μm nightglow emission at Mars with OMEGA/MEX and comparison with general circulation model predictions // J. Geophys. Res. 2012. V. 117. Art.ID. E00J04.

11. *Gérard J.-C., Soret L., Thomas I.R. et al.* Observation of the Mars O_2 visible nightglow by the NOMAD spectrometer onboard the Trace Gas Orbiter // Nature Astronomy. 2024. V. 8. P. 77-81.

12. *Krasnopolsky V.A., Krysko A.A., Rogachev V.N. et al.* Spectroscopy of Venus night sky airglow on Venera-9 and Venera-10 spacecraft // Cosmic Research. 1976. V. 14. No. 5. P. 789-795.

13. *Migliorini A., Piccioni G., Gerard J.C. et al.* The characteristics of the O_2 Herzberg II and Chamberlain bands observed with VIRTIS/Venus Express // Icarus. 1976. V. 223. Iss. 1. P. 609-614.

14. *Broadfoot A.L., Bellaire P.J. Jr.* Bridging the gap between ground-based and space-based observations of the night airglow // J. Geophys. Res. 1999. V. 104. Iss. A8. P. 17127-17138.

15. *Sheese P.E., McDade I.C., Gattinger R.L. et al* . Atomic oxygen densities retrieved from Optical Spectrograph and Infrared Imaging System observations of O_2 A-band airglow emission in the mesosphere and lower thermosphere // J. Geophys. Res. 2011. V. 116. Art.ID. D01303.

16. *Gagne M.-E., Melo S.M.L., Lefevre F. et al.* Modeled O_2 airglow distributions in the Martian atmosphere // J. Geophys. Res. 2012. V. 117. Art.ID. E06005.

17. *Antonenko O.V., Kirillov A.S* . Investigation of the influence of seasonal and latitudinal variations of atomic oxygen on the intensity of intrinsic emission of Earth's and Mars' night atmospheres // Cosmic Research. 2024. V. 62. No. 1. P. 51-59.

18. *Kirillov A.S.* Electronic kinetics of main atmospheric components in high-latitude lower thermosphere and mesosphere // Ann. Geophys. 2010. V. 28. Iss. 1. P. 181−192.

19. *Kirillov A.S.* The calculation of quenching rate coefficients of O_2 Herzberg states in collisions with CO_2, CO, N_2, O_2 molecules // Chem. Phys. Lett. 2014. V. 592. P. 103−108.

20. *Antonenko O.V., Kirillov A.S.* Modeling of Earth's night sky emission spectrum for band systems emitted during spontaneous transitions between different states of electronically excited oxygen molecule // Izv. RAN. Ser. Physical. 2021. V. 85. No. 3. P. 310−314.

21 . *Antonenko O.V., Kirillov A.S.* Modeling of emission intensity of Chamberlain and Herzberg I bands in Earth's night sky and comparison of calculation results with experimental data // Geomagnetism and Aeronomy. 2022. V. 62. No. 5. P. 661–670.

22. *Yankovsky V.* On how atmospheric temperature affects the intensity of oxygen emissions in the framework of the Barth's mechanism // Advances in Space Research. 2021. V. 67. P. 921–929.

23. *Krasnopolsky V.A.* Excitation of the oxygen nightglow on the terrestrial planets // Planet. Space Sci. 2011. V. 59. Iss. 8. P. 754−756.

24. *Bates D.R.* Oxygen band system transition arrays // Planet. Space Sci. 1989. V. 37. Iss. 7. P. 881−887.

25. *Perminov V.I., Semenov A.I., Shefov N.N.* Deactivation of vibrational states of hydroxyl molecules by atomic and molecular oxygen in the mesopause region // Geomagnetism and Aeronomy. 1998. V. 38. No. 6. P. 642−645.

26. *Broadfoot A.L., Kendall K.R.* The Airglow Spectrum, 3100-10,000 A // J. Geophys. Res. 1968. V. 73. Iss. 1. P. 426–428.

27. *Broadfoot A.L., Hunten D.M.* Excitation of N_2 band systems in aurora // Canadian. J. Phys. 1964. V. 42. Iss. 6. P. 1212-1230.

28. *Slanger T.G., Cosby PP.C., Huestis D.L. et al* . Vibrational level distribution of O_2 in the mesosphere and lower thermosphere region // J. Geophys. Res. 2000. V. 105. Iss. D16. P. 20557-20564.

29. *Vogt S.* The High Resolution Echelle Spectrometer on the Keck ten-meter telescope // Opt. Eng. 1994. V. 2198. P. 362-375.

30. *Osterbrock D.E., Fulbright J.P., Martel A.R. et al.* Night-sky high-resolution spectral atlas of OH and O_2 emission lines for echelle spectrograph wavelength calibration // Publ. Astron. Soc. Pacific. 1996. V. 108. P. 277-308.

FIGURE CAPTIONS

Fig.1. Altitude profiles of O concentrations: Panel a - dark lines according to measurements [1] at Earth's middle latitudes for months 1, 4, 7 and 10; light lines - data from NRLMSISE-00 for the same conditions; b - dark lines - data obtained from *TIMED* satellite in Earth's equatorial region (April, August) and northern tropics (autumn, winter) [15]; light lines - data from NRLMSISE-00; c - dark lines data for Mars atmosphere obtained from SPICAM IR spectrometer for orbits at points $Ls \approx 152.1°$, $Ls \approx 164.5°$, 82° S lat. Mars [9]; light lines - data from LMD-MGCM; d - LMD-MGCM data for Mars equatorial region and 67° N lat., for points $Ls \approx 180°$ and $Ls \approx 0°$ [16].

Fig.2. Panel a - experimental data obtained from the space shuttle " *Endeavor* " [14] in the range of 620-900 nm (Atmospheric bands); b - calculated values of integral luminosity of Atmospheric bands for Earth's atmosphere at middle latitudes (55.7° N) for October 1986 ; c - calculated values for Earth's equatorial zone and northern tropics (23° N) for autumn period of 1995 ; d - experimental data from shuttle " *Discovery* ", December 1992 in the range of 300-870 nm (Chamberlain bands); e - calculated values of integral luminosity of Chamberlain bands for Earth's atmosphere at middle latitudes (55.7° N) for October 1986 ; f - calculated values for Earth's equatorial zone and northern tropics (23° N) for autumn period of 1995 .

Fig.3. Panel a - experimental data obtained from the space shuttle " *Endeavor* " [14] in the range of 620-900 nm (Atmospheric bands); b - calculated values of integral luminosity of Atmospheric bands for Mars atmosphere at latitude 67° N at $Ls \approx 180°$.

Fig.4. Panel a - experimental data obtained from EbertFastie spectrograph in the range of 250-370 nm (Kitt Peak Observatory); b - calculated values of integral luminosity of Herzberg I bands for Earth's middle latitudes; c - experimental data obtained from EbertFastie spectrograph in the range of 300-870 nm; d - calculated values of integral luminosity of Chamberlain bands for Earth's middle latitudes.

Fig.5. Panel a - calculated values of Atmospheric bands intensity for Earth's middle latitudes (55.7° N) for January 1986 ; b - measurement data obtained by high-resolution spectrograph (HIRES) on Keck I telescope [28], c - calculation results for equatorial zone including northern tropics (23° N), for winter period of 1995 .

Table 1. Vibrational level energies of five electronically excited states of $O_{2\ \text{molecule}}$

State	Energy E (cm^{-1})
$A\,^3\Sigma_u^+$ ($v = 0 \div v = 11$)	35010 ÷ 40926
$A'\,^3\Delta_u$ ($v = 0 \div v = 11$)	34387 ÷ 40873
$c\,^1\Sigma_u^-$ ($v = 0 \div v = 11$)	32665 ÷ 39360
$b\,^1\Sigma_g^+$ ($v = 0 \div v = 11$)	13122 ÷ 27004
$a\,^1\Delta_g$ ($v = 0 \div v = 11$)	7889 ÷ 22761

Table 2. Coefficients for calculating concentrations of electronically excited oxygen O_2*

		Earth	Mars
M_i		O_2,N_2	CO_2
k_1 ($cm^6\,s^{-1}$)		$k_1 = 6\cdot10^{-34}(300/T)^{2.3}$	$k_1 = 2\cdot2.7_2^{-34}(300/T)$
k_2 ($cm^3\,s^{-1}$)		k_2^{O2}, k_2^{N2}	k_2^{CO2}
O_2*$A\,^3$	$q_{v'}$	0.001÷0.09	0.001÷0.09
	α	0.05	0.05
	$A_{v'}^{A\,3}$ (s^{-1})	15	15
O_2*$A'\,^3$	$q_{v'}$	0.001÷0.09	
	α	0.12	
	$A_{v'}^{A'\,3}$ (s^{-1})	0.87	
O_2*$b\,^1$	$q_{v'}$	0.001÷0.09	0.001÷0.09
	α	0.2	0.2
	$A_{v'}^{b\,1}$ (s^{-1})	0.089	0.089

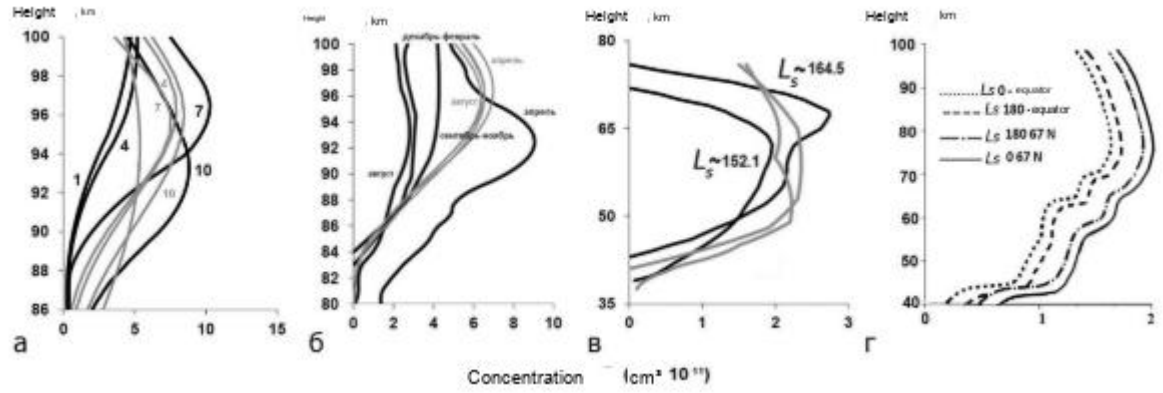
Height , km
а
б
в
г
L_s~164.5
L_s~152.1
Ls 0 - equator
Ls 180 - equator
Ls 180 67 N
Ls 0 67 N
Concentration (cm³ 10 ¹¹)

Fig.1.

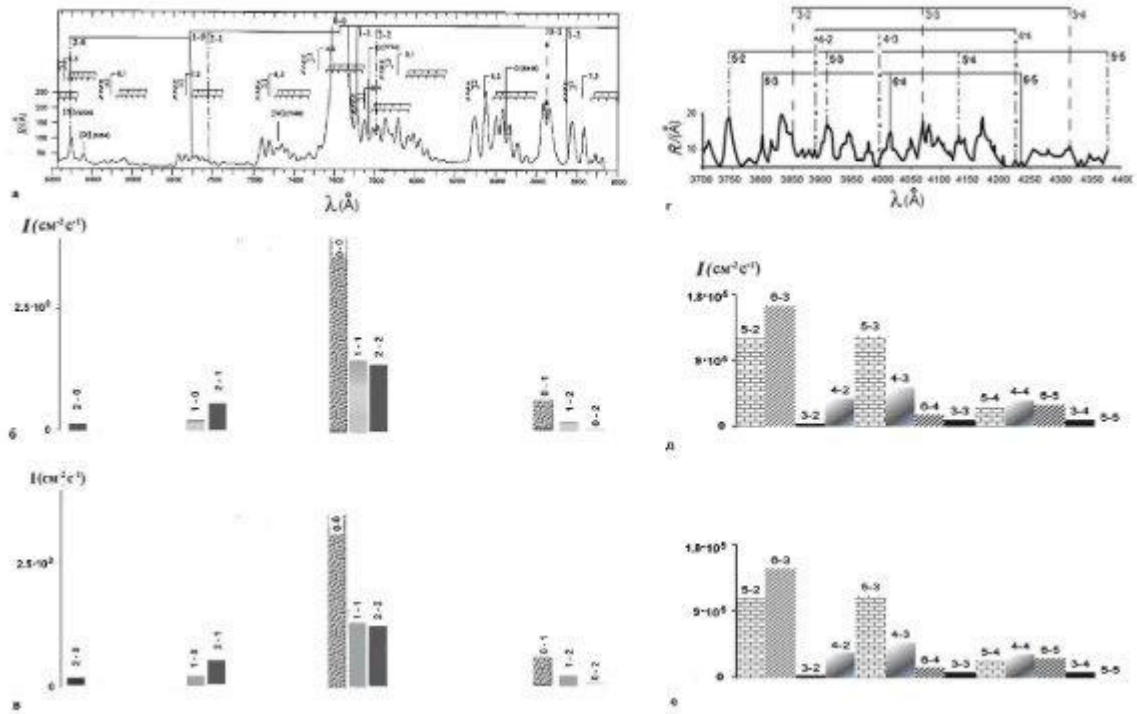
λ(Å)
I(см⁻²с⁻¹)
а
б
в
г
д
е

Fig.2.

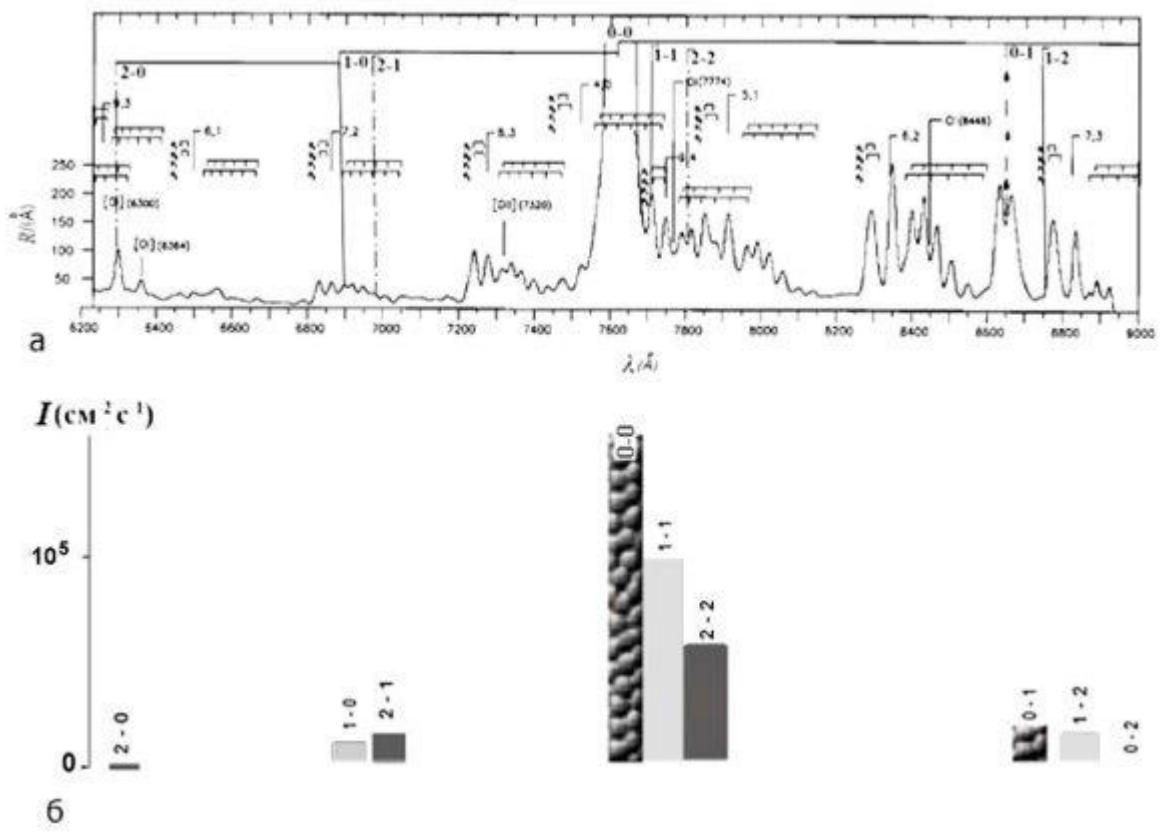
а
λ (Å)
I (см⁻² с⁻¹)
10⁵
0
2 - 0
1 - 0
2 - 1
0 - 0
1 - 1
2 - 2
0 - 1
1 - 2
0 - 2
б

Fig.3.

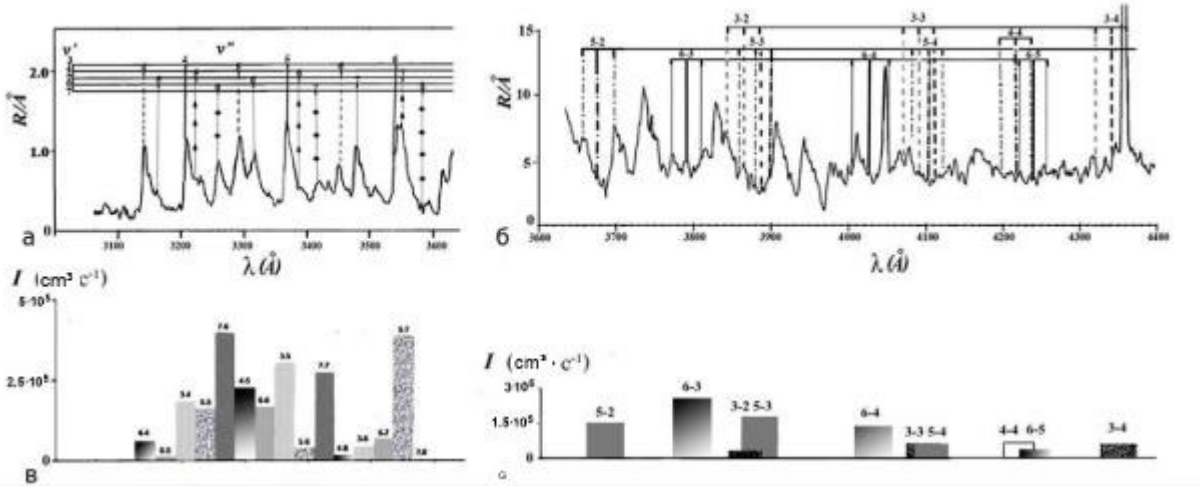
R/Å
а
λ (Å)
б
I (cm³ c⁻¹)
I (cm³ · c⁻¹)
в

Fig.4.

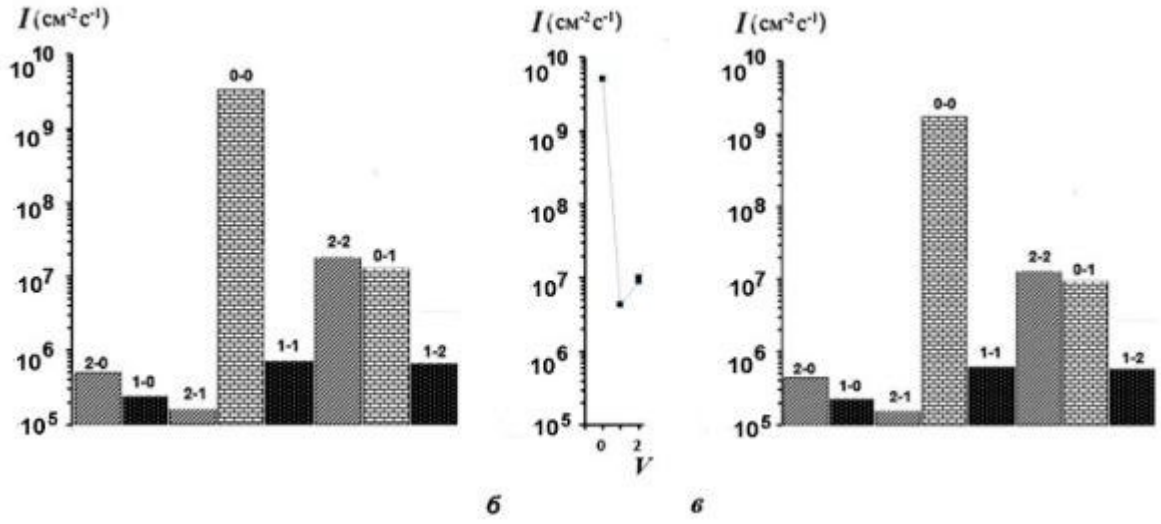

Fig.5.